

Application of K Factors in the $H \rightarrow ZZ^* \rightarrow 4l$ Analysis at the LHC

Kyle Cranmer, Bruce Mellado, William Quayle,
Sau Lan Wu

*Physics Department
University of Wisconsin - Madison
Madison, Wisconsin 53706, USA*

Abstract

Higher order corrections to the Higgs and the non-resonant ZZ production at the LHC are evaluated within the context of the $H \rightarrow 4l$ analysis for Higgs masses $120 < M_H < 180$ GeV. The impact of experimental cuts on the Next-to-Leading Order K factors for Higgs and ZZ production is small. The discovery potential of the $H \rightarrow 4l$ modes is re-evaluated. With the application of conservative higher order corrections the amount of luminosity needed to achieve a 5σ signal significance with the $H \rightarrow 4l$ modes drops by 30 – 35%, depending on the Higgs mass.

1 Introduction

In the Standard Model (SM) of electro-weak and strong interactions, there are 4 types of gauge vector bosons (gluon, photon, W and Z) and 12 types of fermions (six quarks and six leptons) [1]. These particles have been observed experimentally. The SM also predicts the existence of one scalar boson, the Higgs boson [5]. The existence of the Higgs boson remains one of the major cornerstones of the SM.

Nowadays, the observation of the Higgs boson is a primary focus of the ATLAS detector [11]. The Higgs is predominantly produced at the LHC via the gluon-gluon fusion mechanism [12]. The second most important production mechanism is vector boson fusion (VBF) [13]. The inclusion of Higgs searches using dedicated event selections to enhance the contribution from the VBF mechanism has dramatically enhanced the sensitivity of the LHC experiments to low mass Higgs. Early parton level analyses showed that VBF modes could become the most powerful discovery modes in a large range of the Higgs mass, M_H , $115 < M_H < 200 \text{ GeV}$ [15]. More detailed analyses performed by the ATLAS collaboration which include initial and final state gluon radiation, hadronization, multiple interactions and detector effects have confirmed this statement [18] (See Figure 1).

Nevertheless, the $H \rightarrow ZZ^* \rightarrow 4l$, or 4-lepton decay modes ¹ (see the red curve with solid triangles in Figure 1) remain very powerful discovery modes over a wide range of Higgs masses. The appearance of four high transverse momentum, P_T , leptons providing a relatively narrow resonance is an attractive signature experimentally. A relatively large signal to background ratio is provided, as well.

The cross-section for the production Higgs via the gluon-gluon fusion mechanism is subject to strong higher order corrections. The K factor has been computed to Next-to-Next-to Leading Order (NNLO) using the approximation that the top quark mass goes to infinity [19, 20, 21]. The K factor to NNLO for this production mechanism ranges between $1.7 < K < 2.5$, depending on the choice of factorization and renormalization scales and the Higgs mass.

Multivariate techniques could significantly improve the signal significance by conveniently exploiting the angular/momentum correlations between the decay leptons. Multivariate techniques will be applied in a future note ².

In this work we quantify the effect of including higher order corrections to signal and the main background processes on the basis of the classical cut analysis. The starting point of the re-evaluation of the discovery potential of the $H \rightarrow ZZ^* \rightarrow 4l$ modes is the study presented in the ATLAS TDR [11].

¹The dominant contributions arises from gluon-gluon fusion

²In order to perform a multivariate analysis at NLO it is mandatory to implement NLO event generators for the signal and at least the main background processes. For the moment, there exists an NLO event generator only for ZZ production: the MC@NLO event generator [22]. The signal process will be available within this MC event generator in the near future [23].

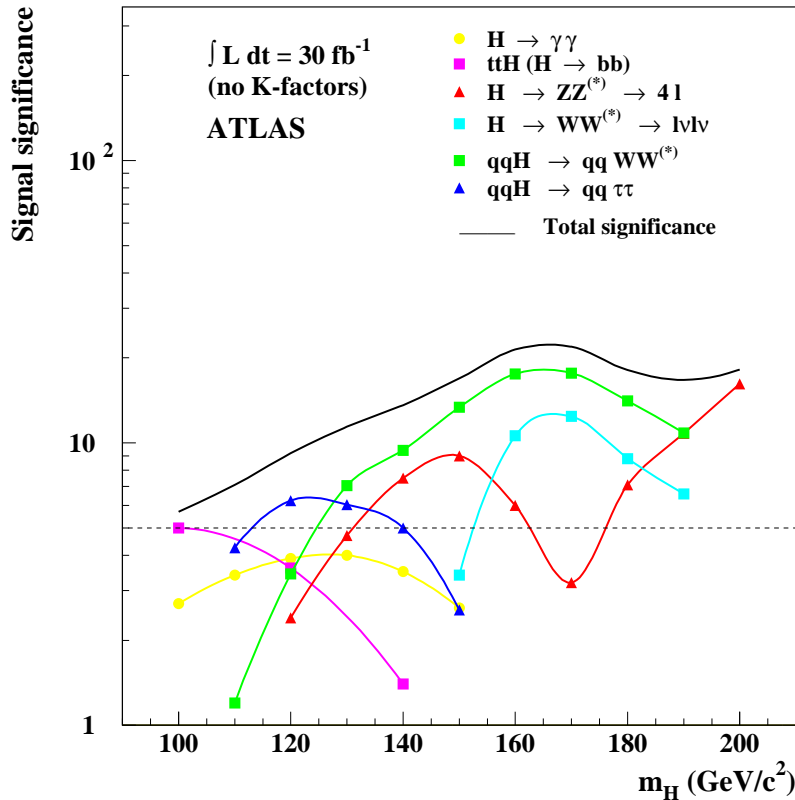


Figure 1: Expected Higgs signal significance obtained with the ATLAS detector with 30fb^{-1} of accumulated luminosity. No K factors have been applied.

2 A Number of Useful Definitions

A lot of effort has been invested for over a decade to estimate QCD higher order corrections to Higgs production in collider facilities. Next-to-Leading Order (NLO) corrections to Higgs production via gluon-gluon fusion are known exactly [24, 27]. NNLO calculations have been made available recently [19, 20, 21]. These calculations were performed in the infinite top mass limit approximation [28, 27]. This approximation is a valid one provided that the Higgs mass and the transverse momentum of the Higgs, P_{TH} , are significantly smaller than the top mass. At the LHC the Higgs is predominantly produced with $P_{TH} < 100\text{GeV}$. The perturbative expansion seems to be converging for LHC energies, which gives us confidence that N^3LO corrections may not play a significant role.

In recent years there has been significant progress in the calculation of higher order corrections to the production of major SM backgrounds in Higgs searches and the development of NLO MC's. The major background in the the searches for

$H \rightarrow ZZ (ZZ^*) \rightarrow 4l$ correspond to the non-resonant production of $ZZ(ZZ^*)$. The NLO corrections to the production of weak vector bosons has been known for over a decade and are of the order of 30%. One would naively expect that NNLO corrections are not of great relevance because of the smallness of the NLO correction. Other SM backgrounds, such as $t\bar{t}$ and $Zb\bar{b}$ production contribute little to the total background in the searches for $H \rightarrow ZZ (ZZ^*) \rightarrow 4l$.

It is convenient to settle on a number of definitions in order to avoid unnecessary confusion. In the theoretical literature the Higgs $K(NLO)$ factor is defined as $K(NLO) = \sigma(NLO)/\sigma(LO)$, where $\sigma(NLO)$ and $\sigma(LO)$ correspond to the total NLO and Leading Order (LO) cross-sections, respectively, evaluated with the strong coupling constant, α_S , and the parton density functions at the corresponding order. In general, these are evaluated when the factorization and the renormalization scales are set to the Higgs mass. Similarly, $K(NNLO) = \sigma(NNLO)/\sigma(LO)$, where $\sigma(NNLO)$ is the NNLO total cross-section.

It should be noted that in the literature the K factors sometimes refer to the higher order corrections to the gluon-gluon fusion mechanism, the dominant Higgs production mechanism. A confusing notation ($pp \rightarrow HX$) is used sometimes to refer to the higher order corrections to this mechanism. However, for Higgs masses $120 < M_H < 190$ GeV the gluon-gluon fusion mechanism does not fully saturate the total Higgs production cross-section at the LHC

Table 1 displays the Leading Order (LO) Higgs cross-section production for the two major production mechanisms at the center of mass energy of the LHC, as calculated with the PYTHIA6.1 program [32]. The contribution from the gluon-gluon fusion and the VBF mechanisms account for $\approx 70\%$ and $18 - 23\%$ of the total Higgs production cross-section, respectively. Additionally, the contribution from VBF to the total cross-section is expected to increase with P_{TH} . The latter is a very important discriminating variable. The ZZ system produced by the decay of the Higgs is expected to display a significantly harder spectrum compared to that of the non-resonant production [34].

In the literature higher order corrections are usually presented for the "fully" inclusive case, after the integration over the kinematics of the particles in the initial and final states. However, these estimates are of little practical use except for "guiding the eye". Experimentally, inclusive searches are performed in a restricted fraction of the phase space. A number of experimental criteria need to be fulfilled before the search may be performed. Restrictions on the transverse momentum and angular acceptance of the Higgs decay products are applied. Isolation of leptons is crucial experimentally.

At this stage it is necessary to establish a clear distinction between a MC integrator and an MC event generator. A MC integrator is capable of applying cuts in the phase space at parton level and also provides meaningful one dimensional distributions. This makes a MC integrator useful when calculating cross-sections in a particular region of the phase space. However, only a MC event generator is able to produce actual events, i.e., the four-momenta of incoming and outgoing particles in the hard interaction. Ide-

$M_H(\text{GeV})$	σ_{VBF}	σ_{gg}	σ_{tot}	$\sigma_{VBF}/\sigma_{tot}$	σ_{gg}/σ_{tot}
120	4.20	17.21	23.96	0.18	0.72
130	3.94	14.80	20.75	0.19	0.72
140	3.61	13.13	18.28	0.20	0.72
150	3.44	11.65	16.35	0.21	0.71
160	3.19	10.46	14.67	0.22	0.71
170	2.95	9.39	13.21	0.22	0.71
180	2.80	8.42	12.04	0.23	0.71

Table 1: Values of the Higgs production Leading Order cross-section (in pb) with the VBF mechanism, σ_{VBF} , and the gluon-gluon fusion mechanism, σ_{gg} , calculated with PYTHIA6.1 for different values of M_H (in GeV). The values of σ_{VBF} and σ_{gg} are compared to the total Higgs cross-section, σ_{tot} .

ally, one would like to have NLO MC event generators to model all processes, as they can easily be interfaced with programs which model other relevant effects, such as hadronization processes, soft and collinear QCD radiation, underlying event, multiple interactions and detector response. Today very few processes in $p - p$ collisions may be modeled with NLO event generators. LO event generators are commonly used for the estimation of the efficiencies (the ratio of the number of events reconstructed in the detector over the total number of events generated), which is a complex convolution of the kinematics of the hard interaction with a number of other effects mentioned above. Higher order corrections are usually applied “by hand”. The effective cross-sections calculated with the help of LO event generators are scaled up with higher order corrections, or the so called K factors. Assuming that the hard interaction and the rest of the relevant effects may be factorized, these K factors may be calculated at parton level.

In order to evaluate the NLO corrections to signal and background after the application of experimental cuts a MC integrator is used. This program helps evaluate the “experimental” higher order correction which is referred here to as $K_{CUTS}(NLO)$:

$$K_{CUTS}(NLO) = \frac{\int_{CUTS} \frac{d\sigma(NLO)}{d\Phi} d\Phi}{\int_{CUTS} \frac{d\sigma(LO)}{d\Phi} d\Phi}. \quad (1)$$

The integration of the differential cross-section is performed over the phase space, Φ , as defined by the event selection performed experimentally.

At present, no NLO event generator is available for Higgs production at the LHC. Fortunately enough, we have at our disposal a MC integrator that is able to apply cuts in the phase space at the parton level. Detector effects may not be an issue as long as the experimental cuts are soft enough with respect to the kinematics of the final state partons. This is the case for the inclusive search $H \rightarrow ZZ^* \rightarrow 4l$ (see Sections 3 and 4.1).

The MC integrator MCFM [35] is used for the evaluation of $K_{CUTS}(NLO)$ for the Higgs signal ³ and the ZZ production. Exact matrix elements containing the leptonic decays are implemented in this program.

The analysis presented in the ATLAS TDR [11] was based on LO matrix element (ME) interfaced with the initial and final state radiation (IFSR), or parton shower (PS), provided within the PYTHIA package. Strictly speaking, the resulting final state does not correspond to LO due to the presence of hard jets radiated by the IFSR. The total LO cross-section is left unchanged by the IFSR, however, the kinematics of the final state will be, generally speaking, different from a LO final state. The kinematics of the final state are expected to be affected little by the soft and collinear radiation.

One would like to have an event generator in which the NLO ME is interfaced with IFSR in order to provide proper treatment of divergences while avoiding double counting [37, 38]. Unfortunately, such type of MC event generators are still unavailable for signal production. In order to get around that a simple procedure is defined here to estimate the impact of hard IFSR on the kinematics of the LO final state. The factor $\epsilon_{CUTS}(PS)$ is defined as:

$$\epsilon_{CUTS}(PS) = \frac{\int_{CUTS} \frac{d\sigma_{PS}(LO)}{d\Phi} d\Phi}{\int_{CUTS} \frac{d\sigma(LO)}{d\Phi} d\Phi}, \quad (2)$$

where $\sigma_{PS}(LO)$ corresponds to the cross-section obtained with the LO ME after the application of IFSR. The integration of the differential cross-section is performed over the phase space, as defined by the event selection performed experimentally. The factor $\epsilon_{CUTS}(PS)$ may be evaluated at the parton level with the help of LO ME interfaced with IFSR provided by PYTHIA. This factor does not have real physical meaning by itself. Nevertheless, it proves a useful consistency check.

As long as $\epsilon_{CUTS}(PS)$ is relatively close to unity one can safely re-write the NLO cross-section as:

$$\sigma^*(NLO) \approx K_{CUTS}(NLO)/\epsilon_{CUTS}(PS) \cdot \sigma^*(LO), \quad (3)$$

and

$$\sigma^*(LO) = \int_{CUTS} \left(\frac{d\sigma(LO)}{d\Phi} \oplus PS \oplus HAD \oplus UE \oplus MI \oplus DE \right) d\Phi, \quad (4)$$

where $\sigma^*(LO)$ corresponds to the LO cross-section convoluted with the parton shower, effects of hadronization (HAD), underlying event (UE), multiple interactions (MI) and detector acceptance and efficiency (DE). The TDR analysis quotes $\sigma^*(LO)$, which we are going to use as input to Equation 3.

³MCFM implements the NLO ME for Higgs production using the approximation that the top quark mass goes to infinity. The cross-sections obtained with MCFM without experimental cuts are consistent with the program HIGLU [36].

3 The TDR Event Selection

As pointed out in the introduction, the goal of the present note is to re-evaluate the classical cut analysis presented in the ATLAS TDR [11] by applying NLO corrections to both signal and the major backgrounds.

The event selection applied in the ATLAS TDR [11], which is based on [39, 40, 41], consists of the following cuts:

- At least two leptons with $P_T > 20 \text{ GeV}$.
- All leptons should have $P_T > 7 \text{ GeV}$.
- Leptons are required to be isolated. Stringent isolation criteria allows to suppress the $t\bar{t}$ and $Zb\bar{b}$ background below 10% of the total irreducible background [11].
- Cuts on the invariant mass of same-flavor and opposite-sign leptons. The invariant mass of one couple of leptons is required to be close to the Z mass. The other couple of leptons needs to have an invariant mass larger than a certain threshold. The value of this threshold is a function of the Higgs mass [11].

The signal efficiency was calculated as a function of the background rejection with the help of a full simulation [41]. Table 2 shows the expected number of signal and background events with 30 fb^{-1} of accumulated luminosity, as reported in the ATLAS TDR [11]. After the application of isolation cuts the contribution from $t\bar{t}$ and $Zb\bar{b}$ production (two leptons are produced via the semi-leptonic decay of the b quarks) turns out to be negligible. Efficient suppression of the $t\bar{t}$ and $Zb\bar{b}$ background with lepton isolation selection will represent the most relevant experimental challenge for the signal observability with this analysis. The background is dominated by the production of four leptons from the decay of non-resonant ZZ^* and ZZ .

	120	130	150	170	180
Signal	4.1	11.4	26.8	7.6	19.7
$t\bar{t}$	0.01	0.02	0.03	0.02	0.02
$Zb\bar{b}$	0.08	0.12	0.19	0.17	0.19
ZZ^*	1.23	2.27	2.51	2.83	2.87
$ZZ \rightarrow \tau\tau ll$	0.13	0.20	0.25	0.08	0.02

Table 2: Expected signal and background events with 30 fb^{-1} of accumulated luminosity in the $H \rightarrow ZZ^* \rightarrow 4l$ analysis, as reported in the ATLAS TDR.

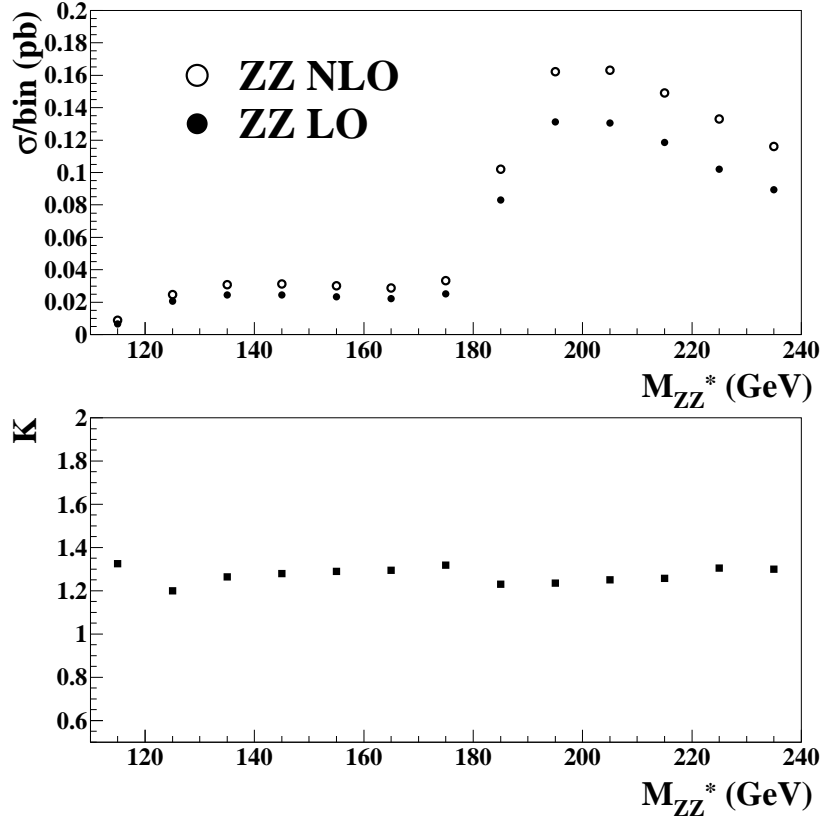


Figure 2: NLO corrections to non-resonant ZZ^* production. The upper plot displays the comparison between the NLO and LO cross-sections (in pb) as a function of the invariant mass of the vector bosons. The lower plot shows the $K(NLO)$ factor as a function of the same variable.

4 Application of NLO Corrections

NLO corrections are applied on the signal, ZZ^* and ZZ production. The remaining background processes are scaled up by a factor of two, in the spirit of a conservative analysis. The NLO corrections to both processes are known, however no NLO MC event generator is available that incorporates the corresponding NLO ME. By scaling the $t\bar{t}$ and $Zb\bar{b}$ LO cross-sections we hope to remain on the conservative side.

There is a great deal of freedom in choosing the normalization of the NLO signal cross-section. A conservative estimation of the scale dependence of the NLO and NNLO signal cross-sections has been performed in [19]. The renormalization and factorization scales were changed in opposite directions, yielding stronger scale dependence of the signal cross-section for the NNLO calculation. As a conservative estimate, the NLO

cross-section is chosen to match the lower bound of the NNLO cross-section ⁴. The lower bound of the NLO band lies well outside the NNLO band, which is supposed to contain the "true" production cross-section. The first row in Table 3 shows the values of the NLO corrections to the cross-section for the gluon-gluon fusion mechanism as a function of the Higgs mass.

As pointed out in Section 2, the gluon-gluon mechanism does not fully saturate the total Higgs cross-section production at the LHC. The VBF cross-section is scaled up by 10% in order to take into account the NLO correction [42]. The rest of the Higgs production mechanisms have not been corrected. Their contribution to the total cross-section remains within the few % level. The resulting values total signal $K(NLO)$ used in this note are given in the second row of Table 3.

	120	130	150	170	180
$K_{gg}(NLO)$	1.74	1.76	1.80	1.84	1.86
$K(NLO)$	1.47	1.47	1.50	1.53	1.54
$K_{CUTS}(NLO)$	1.41	1.43	1.46	1.48	1.50

Table 3: Values of the signal NLO correction factors for signal production as a function of the Higgs mass. $K_{gg}(NLO)$ is the NLO correction factor to the gluon-gluon fusion production mechanism. The values of $K_{CUTS}(NLO)$ obtained with MCFM are shown in the third row (see Section 4.1).

The analysis presented in [41] corrected the LO non-resonant ZZ cross-section by applying a factor of 1.3, in order to take account of the contribution of $gg \rightarrow ZZ$. MCFM does not provide the matrix elements corresponding to the non-resonant $gg \rightarrow ZZ$ production. In this Note we apply the $K(NLO)$ factor on the non-resonant ZZ cross-section presented in [41] (including the application of the factor of 1.3 mentioned above).

The $K(NLO)$ for non-resonant ZZ^* and ZZ productions are expected to be insensitive to the invariant mass of the vector boson pair. The upper plot in Figure 2 displays the comparison between the NLO and LO cross-sections as a function of the invariant mass of the vector bosons. The lower plot shows the $K(NLO)$ factor as a function of the same variable. Additionally, as will be seen in Section 4.1, the effect on the NLO corrections of the cuts on the lepton transverse momentum is small. Therefore, it is safe to use the same $K(NLO)$ factor to correct the LO cross-section of $ZZ \rightarrow \tau\tau ll$ production as the one used for ZZ^* production. The scale uncertainty associated to the NLO correction to this process due to the scale dependence is less than 5% ⁵.

⁴The lower band of the NNLO cross-sections is approximated to a straight line, $K_{gg}(NLO) = 1.7 + 2 \cdot 10^{-3} \cdot (M_H - 100)$, where M_H is expressed in GeV.

⁵It should be noted that in this check the renormalization and factorization scales were set to be equal. This may lead to the underestimation of the scale dependence, although this effect is expected to be small compared with the gluon-gluon fusion Higgs production mechanism.

4.1 Effect of Event Selection on NLO Corrections

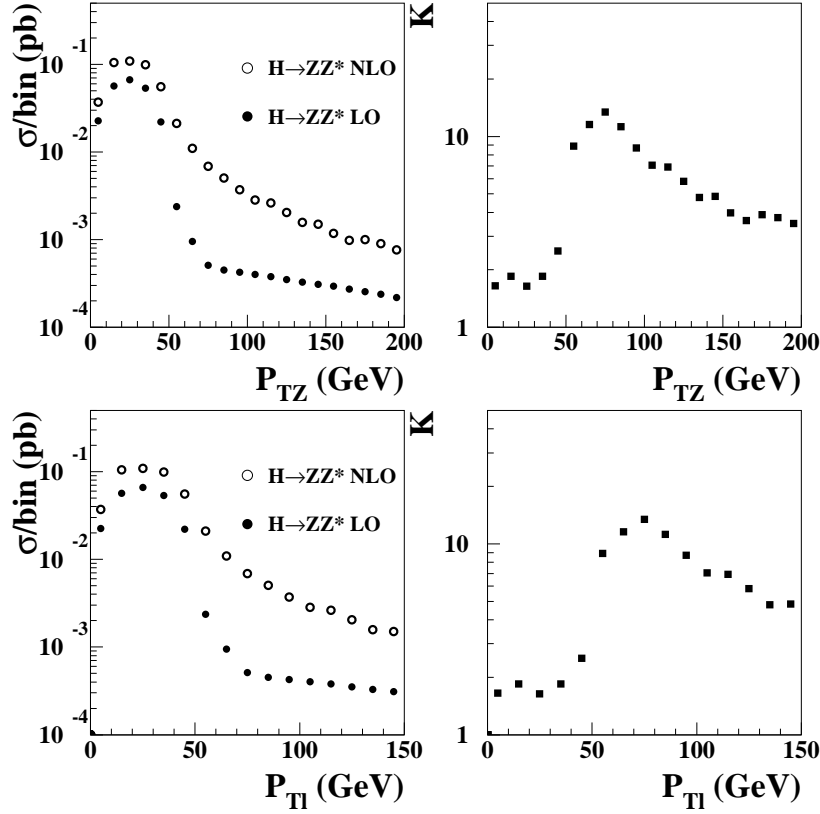


Figure 3: $Z(Z^*)$ boson and lepton transverse momentum distributions with LO and NLO $gg \rightarrow H \rightarrow ZZ^* \rightarrow 4l$ ME's, as evaluated with MCFM. The upper left and right plots show the transverse momentum of the $Z(Z^*)$'s (solid and open circles correspond to LO and NLO, respectively) and the corresponding K factor as a function of the transverse momentum of the $Z(Z^*)$'s. Similarly, the lower plots correspond to the transverse momentum of the leptons. Here, $M_H = 150$ GeV.

As discussed in Section 2, the evaluation of the effect of cuts applied experimentally on the higher order corrections is a mandatory step. This involves the calculation of $K_{CUTS}(NLO)$ in Equation 1. This is effectively done by the MCFM MC integrator for signal and the ZZ^* background.

Figure 3 displays the $Z(Z^*)$ boson and lepton transverse momentum distributions with LO and NLO $gg \rightarrow H \rightarrow ZZ^* \rightarrow 4l$ ME's, as evaluated with MCFM. The upper left and right plots show the transverse momentum of the $Z(Z^*)$'s (solid and open circles correspond to LO and NLO, respectively for $M_H = 150$ GeV) and the corresponding K factor as a function of the transverse momentum of the $Z(Z^*)$'s. Similarly, the lower plots correspond to the transverse momentum of the leptons.

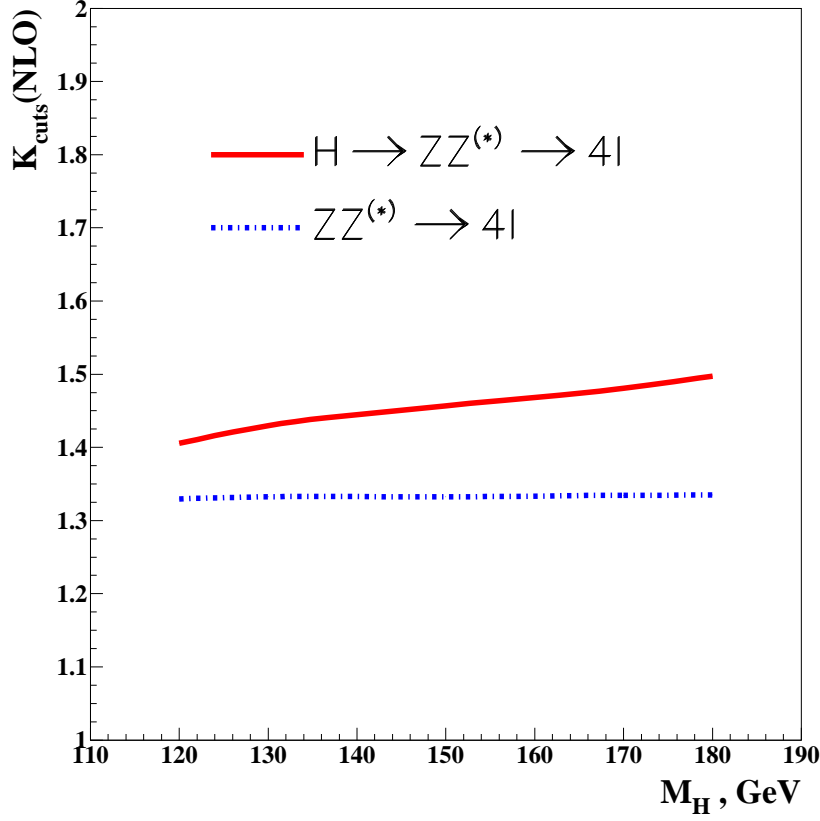


Figure 4: Values of $K_{cuts}(NLO)$ for signal and the ZZ^* background are presented as a function of the Higgs mass (in the case of the ZZ^* production, one considers the invariant mass of the vector boson pair).

The kinematic effect of additional hard partons in the final state shows up at large values of the transverse momentum of the $Z(Z^*)$'s and leptons. In the kinematic region where the cuts on the lepton transverse momentum are applied $K(NLO)$ is basically flat. Hence, the effect of experimental cuts on the NLO corrections is expected to be small for the signal process. The situation is similar for the main background processes.

The values of $K_{cuts}(NLO)$ for signal and the ZZ^* background are presented as a function of the Higgs mass (in the case of the ZZ^* production one considers the invariant mass of the vector boson pair) in Figure 4. The effect of cuts is rather small in the present analysis. It reduces the signal NLO cross-section with respect to the LO cross-section by $\approx 5\%$. The values of $K_{cuts}(NLO)$ in Table 3 may be compared with $K(NLO)$ for signal. This effect in the ZZ^* background is less than 1%.

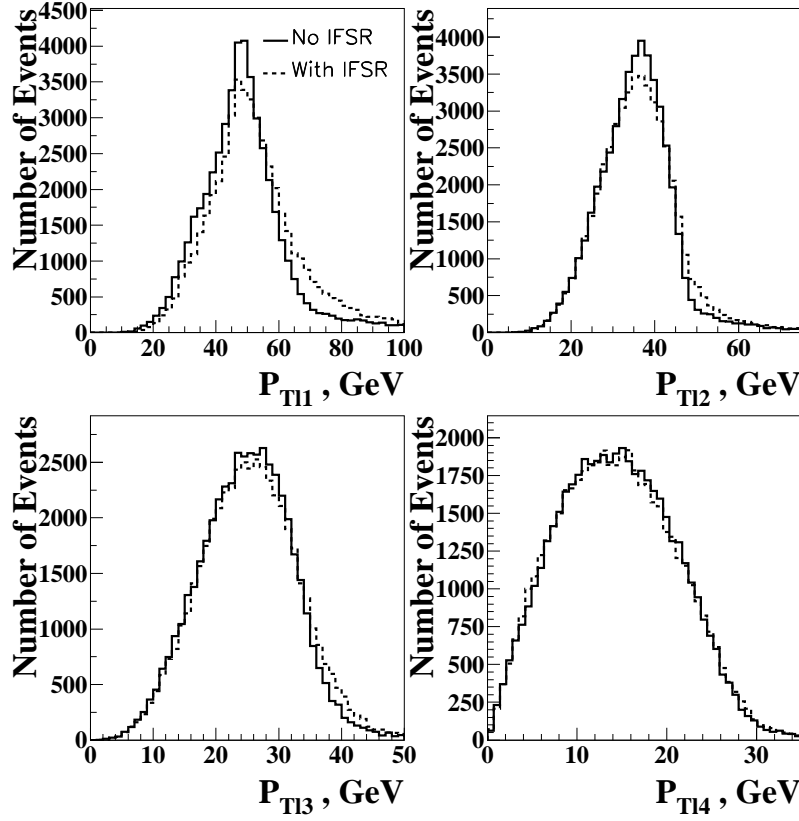


Figure 5: Lepton transverse momentum distribution in $H \rightarrow ZZ^* \rightarrow 4l$ with $M_H = 150$ GeV. Leptons are ordered in P_T . The solid line corresponds to the parton level information as produced by the LO MC without the application of hadronization, parton showers and multiple interaction effects. The dashed lines correspond to the same LO MC after the application of the parton showers. Here, PYTHIA6.1 is used.

4.2 Effect of Hard IFSR

In the previous Section it has been shown that the presence of additional hard partons in the final state has little effect on the kinematics of relatively soft leptons. The effect of hard IFSR on the analysis reported in the ATLAS TDR may be negligible, as the parton shower approach is expected to underestimate the rate of hard additional partons

The solid lines in Figure 5 display the transverse momentum distribution of the leptons, ordered in P_T in $H \rightarrow ZZ^* \rightarrow 4l$ with $M_H = 150$ GeV (LO MC parton level information without the application of hadronization, parton showers and multiple interaction effects). The dashed lines in Figure 5 correspond to the LO MC after the application of IFSR. The effect of hard IFSR is relevant to hard leptons, however, it affects little the P_T region where the experimental cuts are applied. The pseudorapidity

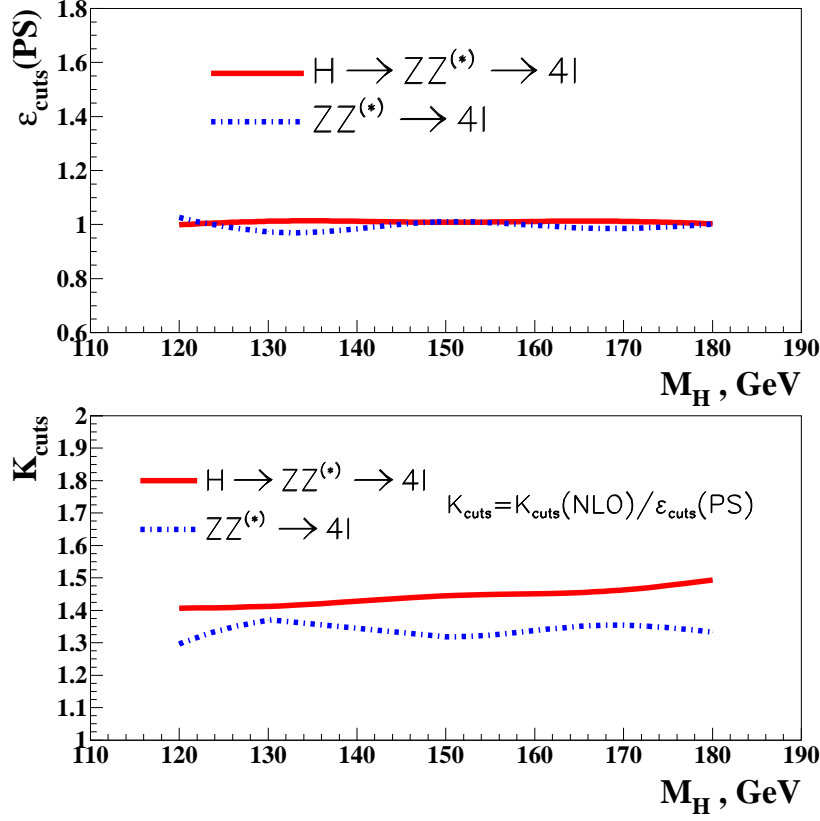


Figure 6: Values of $\epsilon_{CUTS}(PS)$ for signal and the ZZ^* background are presented as a function of the Higgs mass (in the case of the ZZ^* production, one considers the invariant mass of the vector boson pair).

distributions of the leptons are almost unaffected by the IFSR.

The values of $\epsilon_{CUTS}(PS)$, as defined in Equation 2, are consistent with unity within statistical errors, both for signal and the ZZ^* background. This is illustrated in Figure 6. For practical purposes, the final corrected cross-section in Equation 3 for signal and the ZZ^* background are approximated by $\sigma^*(NLO) \approx K_{CUTS}(NLO) \cdot \sigma^*(LO)$ ⁶.

5 Results

In this Section the sensitivity of the ATLAS experiment to SM Higgs with the inclusive search with the $H \rightarrow ZZ^* \rightarrow 4l$ modes is re-evaluated. The cross-sections reported in the ATLAS TDR [11] have been corrected according to Equation 3 following the procedure explained in Section 4.

⁶It should be noted that this conclusion does not generally apply to other inclusive analyses.

Table 4 shows the signal and background effective cross-section before and after the application of NLO corrections. Shown in Table 4 are the signal and background effective cross-sections, the simple event counting Poisson [43] signal significance with 10 and 30 fb⁻¹ of accumulated luminosity (σ_P^{10} and σ_P^{30} , respectively) and the amount of luminosity needed for a 5 σ signal significance, $L^{5\sigma}$. The last row in Table 4 illustrates the reduction of the $L^{5\sigma}$ due to the application of NLO corrections. The amount of luminosity needed to achieve a 5 σ signal significance decreases by 30 – 35%, depending on the Higgs mass.

		120	130	150	170	180
No K factors	S	0.14	0.38	0.89	0.25	0.66
	B	0.05	0.09	0.10	0.10	0.10
	S/B	2.83	4.37	8.99	2.45	6.35
	σ_P^{10}	0.45	2.25	4.80	1.25	3.63
	σ_P^{30}	2.02	4.55	8.88	3.00	6.90
	$L^{5\sigma}$	124.89	35.38	10.68	73.22	16.81
With K factors	S	0.19	0.54	1.30	0.38	0.98
	B	0.07	0.12	0.14	0.14	0.14
	S/B	2.90	4.56	9.48	2.64	6.90
	σ_P^{10}	0.94	2.92	6.00	1.81	4.70
	σ_P^{30}	2.64	5.66	10.92	3.86	8.75
	$L^{5\sigma}$	87.26	24.27	7.29	47.39	11.05
Reduction in $L^{5\sigma}$	$1 - L_{WK}^{5\sigma}/L_{NK}^{5\sigma}$	0.30	0.31	0.32	0.35	0.34

Table 4: Sensitivity of the ATLAS detector to the SM Higgs with the $H \rightarrow ZZ^* \rightarrow 4l$ modes before and after the application of NLO corrections as a function of the Higgs mass. Shown are the signal and background effective cross-sections (in fb), the simple event counting signal significance with 10 and 30 fb⁻¹ of accumulated luminosity (σ_P^{10} and σ_P^{30} , respectively) and the amount of luminosity needed for a 5 σ signal significance, $L^{5\sigma}$. The last row illustrates the reduction of the $L^{5\sigma}$ due to the application of NLO corrections ($L_{WK}^{5\sigma}, L_{NK}^{5\sigma}$ correspond to $L^{5\sigma}$ with and without the K factors, respectively).

Figures 7-8 display the SM Higgs Signal significance expected with the ATLAS detector with the $H \rightarrow ZZ^* \rightarrow 4l$ modes for 10 and 30 fb⁻¹ of accumulated luminosity, respectively. Figure 9 displays the so called luminosity plot. This plot shows the amount of luminosity needed to achieve a 5 σ signal significance with the ATLAS detector with the $H \rightarrow ZZ^* \rightarrow 4l$ modes as a function of the Higgs mass.

A number of improvements needs to be performed in the future. The application of the NLO corrections has been performed without re-optimizing the event selection. New, more accurate, parameterizations of the background rejection and the signal efficiency will be available in the future. This will be a proper time to re-optimize the event selection.

With the appearance in the near future of NLO event generators for the signal process it will be possible to perform more sophisticated multivariate analyses. The multivariate analyses will take advantage of the angular correlations between the leptons, not fully exploited in the past by the classical cuts analyses.

As pointed out in Section 2, the transverse momentum of the four lepton system may become a powerful discriminating variable. Theoretical calculations of P_{TH} based on NLO calculations with the addition of re-summation to all orders are becoming available [44]. These calculations show that the four lepton spectrum of the signal is significantly harder than for the main background.

6 Acknowledgments

We would like to acknowledge J. Campbell for most useful discussions and his invaluable help with the MCFM program. We would also like to thank A. Djouadi, S. Frixione, M. Grazzini, R. Harlander, I. Hinchliffe, E. Richter-Was, M. Spira and H. Zobernig for most useful discussions on higher order corrections to Higgs production at the LHC.

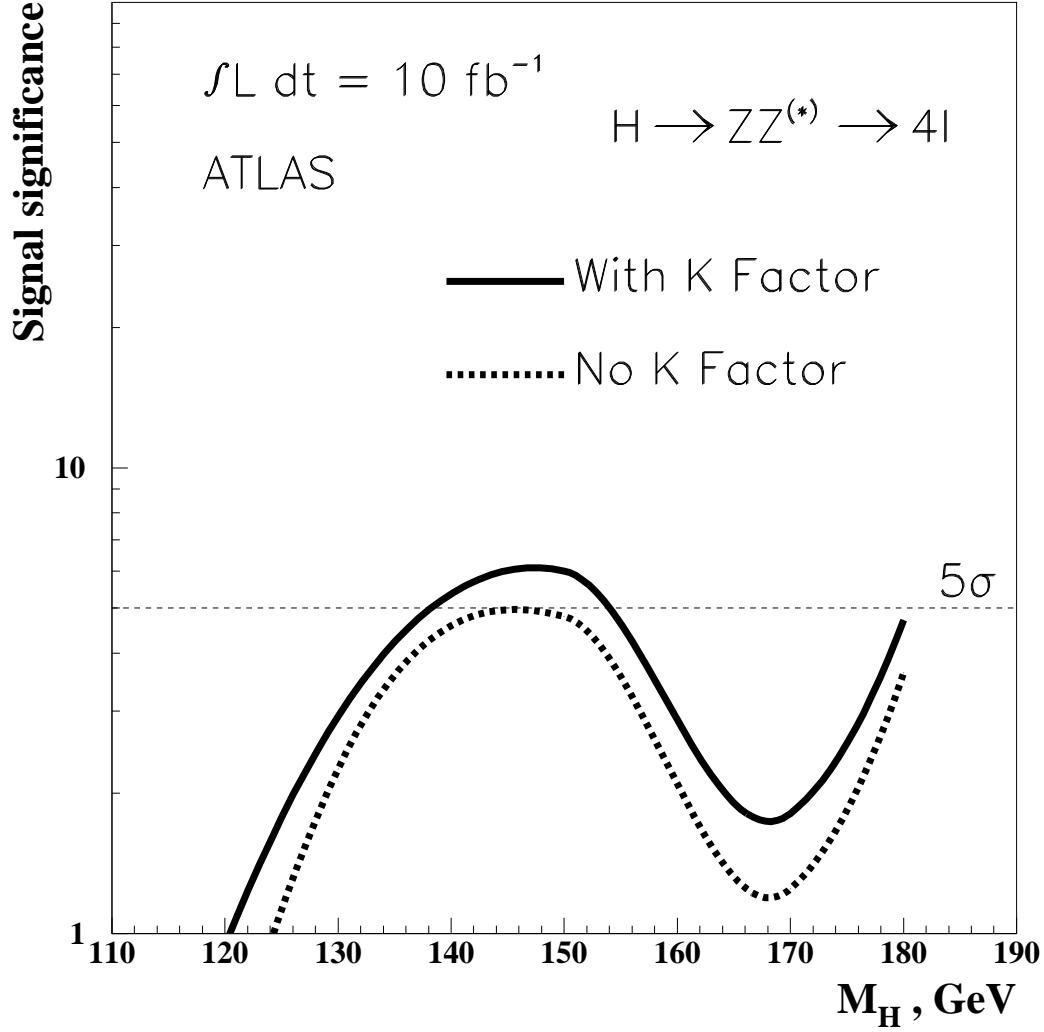


Figure 7: SM Higgs Signal significance expected with the ATLAS detector with the $H \rightarrow ZZ^* \rightarrow 4l$ modes for 10 fb^{-1} of accumulated luminosity as a function of the Higgs mass. The dashed and solid curves correspond to the signal significance before and after the application of NLO corrections, respectively.

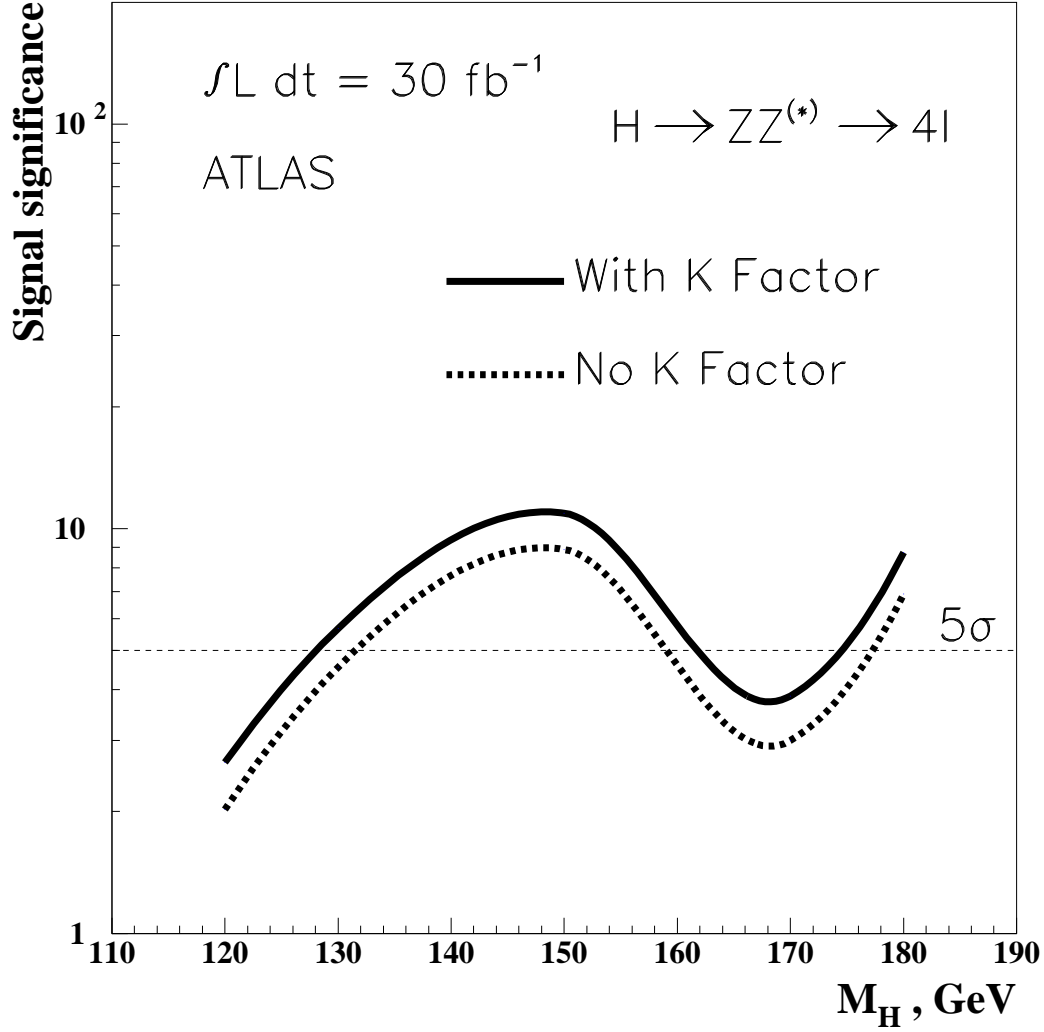


Figure 8: SM Higgs Signal significance expected with the ATLAS detector with the $H \rightarrow ZZ^* \rightarrow 4l$ modes for 30 fb^{-1} of accumulated luminosity as a function of the Higgs mass. The dashed and solid curves correspond to the signal significance before and after the application of NLO corrections, respectively.

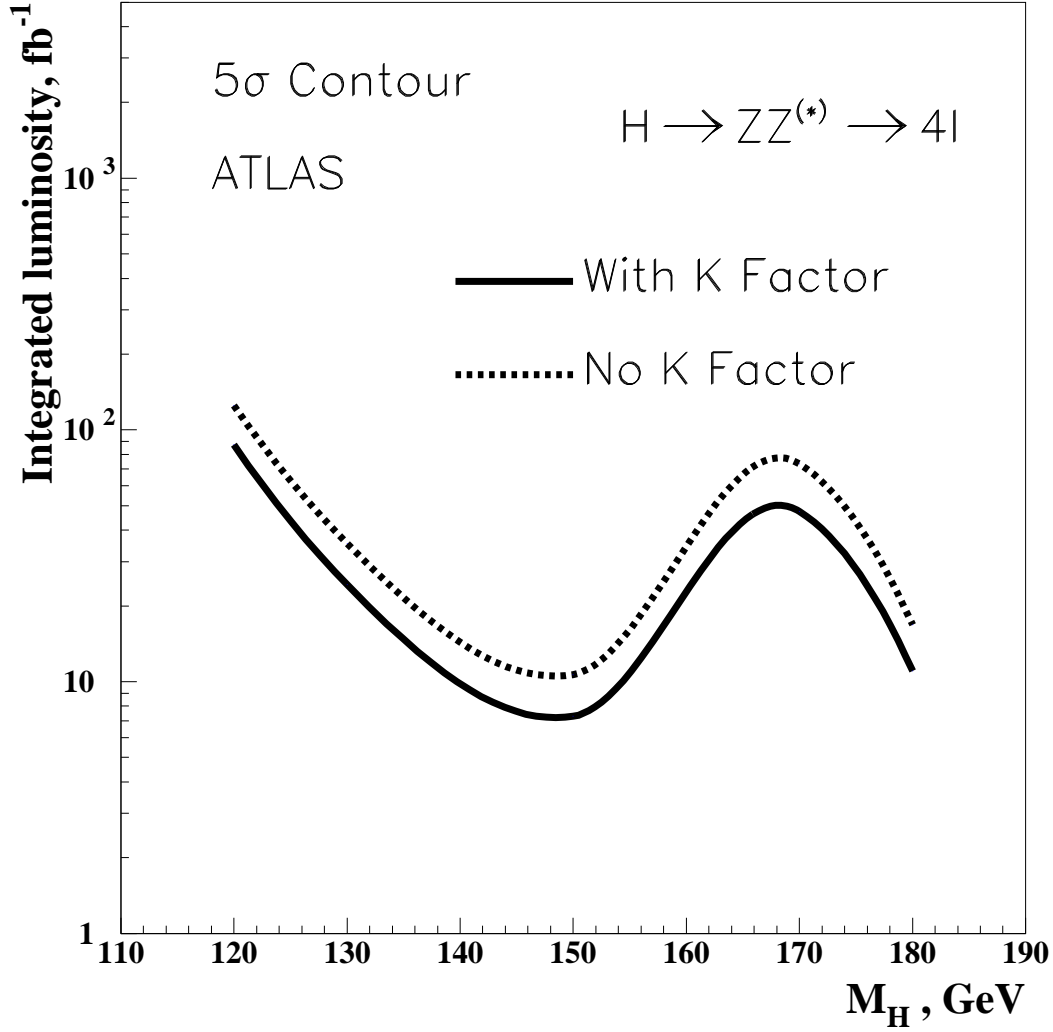


Figure 9: Amount of luminosity needed to achieve a 5σ signal significance with the ATLAS detector with the $H \rightarrow ZZ^* \rightarrow 4l$ modes as a function of the Higgs mass. The dashed and solid curves correspond to the signal significance before and after the application of NLO corrections, respectively.

References

- [1] S. L. Glashow, Nucl. Phys. **B22** (1961) 579
- [2] S. Weinberg, Phys. Rev. Lett. **19** (1967) 1264
- [3] A. Salam, Proceedings to the Eighth Nobel Symposium, May 1968, ed: N. Svartholm (Wiley, 1968) 357
- [4] S.L. Glashow, J. Iliopoulos and L. Maiani, Phys. Rev. **D2** (1970) 1285
- [5] P. W. Higgs, Phys. Lett. **12** (1964) 132
- [6] P. W. Higgs, Phys. Rev. Lett. **13** (1964) 508
- [7] P. W. Higgs, Phys. Rev. **145** (1966) 1156
- [8] F. Englert, R. Brout, Phys. Rev. Lett. **13** (1964) 321
- [9] G. S. Guralnik, C.R. Hagen and T.W.B. Kibble, Phys. Rev. Lett. **13** (1964) 585
- [10] T.W.B. Kibble, Phys. Rev. **155** (1967) 1554
- [11] ATLAS Collaboration, Detector and Physics Performance Technical Design Report, CERN-LHCC/99-14 (1999)
- [12] H. M. Georgi, S. L. Glashow, M. E. Machacek and D. V. Nanopoulos, Phys. Rev. Lett. **40** (1978) 11
- [13] R. Cahn and S. Dawson, Phys. Lett. **B136** (1984) 196
- [14] G. Kane, W. Repko and W. Rolnick, Phys. Lett. **B148** (1984) 367
- [15] D. Rainwater and D. Zeppenfeld, Phys. Rev. **D60** (1999) 113004
- [16] N. Kauer et al., Phys. Lett. **B503** (2001) 113
- [17] T. Plehn, D. Rainwater and D. Zeppenfeld, Phys. Rev. **D61** (2000) 093005
- [18] S. Asai et al., Search for the Standard Model Higgs Boson in ATLAS using Vector Boson Fusion, ATLAS Internal Note ATL-PHYS-2003-005 (2003)
- [19] R. V. Harlander and W. B. Kilgore, Phys. Rev. Lett. **88** (2002) 201801
- [20] C. Anastasiou and K. Melnikov, Nucl. Phys. **B646** (2002) 220
- [21] V. Ravindran, J. Smith and W. L. van Neerven, hep-ph/0302135 (2003)
- [22] S. Frixione and B. R. Webber, The MC@NLO Event Generator, hep-ph/0207182
- [23] S. Frixione, private communication

- [24] S. Dawson, Nucl. Phys. **B359** (1991) 283
- [25] A. Djouadi, M. Spira and P. M. Zerwas, Phys. Lett. **B264** (1991) 440
- [26] D. Graudenz, M. Spira and P. M. Zerwas, Phys. Rev. Lett. **70** (1993) 1372
- [27] M. Spira, A. Djouadi, D. Graudenz and P. M. Zerwas, Nucl. Phys. **B453** (1995) 17
- [28] J. Ellis, M. K. Gaillard, D. V. Nanopoulos, Nucl. Phys. **B106** (1976) 292
- [29] A. I. Vainshtein et al., Sov. J. Nucl. Phys. **30** (1979) 1368
- [30] A. I. Vainshtein et al., Sov. Phys. Usp. **23** (1980) 429
- [31] M. B. Voloshin, Sov. J. Nucl. Phys. **44** (1986) 478
- [32] T. Sjöstrand, Comp. Phys. Comm. **82** (1994) 74
- [33] T. Sjöstrand et al., Comp. Phys. Comm. **135** (2000) 238
- [34] B. Mellado, Higher Order Corrections in $H \rightarrow ZZ^* \rightarrow 4l$, presentation given at the Higgs working group meeting on 10/03/03
- [35] J. Campbell and K. Ellis, Phys. Rev. **D60** (2002) 113006
- [36] M. Spira, HIGLU: A Program for the Calculation of the Total Higgs Production Cross Section at Hadron Colliders via Gluon Gluon Fusion Including QCD Corrections, DESY T-95-05, hep-ph/9510347 (1995)
- [37] S. Frixione and B. R. Webber, JHEP **0206** (2002) 029
- [38] Y. Kurihara et al., Nucl. Phys. **B654** (2003) 301
- [39] L. Guyot, D. Froidevaux and L. Poglioli, Physics Performance for Various Muon System Configurations, ATLAS internal Note ATL-PHYS-1995-076 (1995)
- [40] O. Linossier and L. Poglioli, Final State Inner-Bremsstrahlung Effects on $H \rightarrow ZZ^* \rightarrow 4l$ Channel with ATLAS, ATLAS internal Note ATL-PHYS-1995-075 (1995)
- [41] O. Linossier and L. Poglioli, H to ZZ^* to Four Leptons Channel in ATLAS. Signal Reconstruction and Reducible Background Rejection, ATLAS internal Note ATL-PHYS-1997-101 (1997)
- [42] T. Han, G. Valencia and S. Willenbrock, Phys. Rev. Lett. **69** (1992) 3274
- [43] K. Cranmer, B. Mellado, W. Quayle and Sau Lan Wu, Confidence Level Calculations in the Search for Higgs Bosons Decay $H \rightarrow W^+W^- \rightarrow l^+l^- \cancel{p}_T$ Using Vector Boson Fusion, ATLAS internal Note ATL-PHYS-2003-008 (2003)
- [44] G. Bozzi et al., The q_T Spectrum of the Higgs Boson at the LHC in QCD Perturbation Theory, hep-ph/0302104.